A deep learning approach to denoise luminescence images of solar cells

Grace Liu[1], Priya Dwivedi[1], Thorsten Trupke[1] and Ziv Hameiri[1]

[1]*University of New South Wales (UNSW), Sydney NSW 2052, Australia*

Abstract—Luminescence imaging is essential for solar cell performance and reliability analysis. It is used to identify spatial defects and extract key electrical parameters. To reliably identify defects, high quality images are desirable, however, acquiring such images implies a higher cost and/or lower throughput as they require better imaging systems and/or longer exposure times (as using cheaper cameras or reducing the exposure time often increases the amount of noise). Therefore, this study proposes a deep learning model to significantly reduce the noise in electroluminescence images, hence, improving their quality without the need for additional hardware expenses or longer exposure times. The proposed deep learning approach improved noisy images by 30.4% and 39.3% in terms of the peak signal-to-noise ratio and the structural similarity index, respectively.

Introduction

To reach the Paris climate goals, the international renewable energy agency (IRENA) states that the total solar photovoltaic (PV) capacity must reach almost 18 times the 2018 levels by 2050 [1]. A promising method to support this massive growth is through improving the efficiency of PV manufacturing using machine learning.

Electroluminescence (EL) imaging is a powerful method to inspect solar cells and modules [2]. When an electrical current is injected into a solar cell, luminescence is emitted [3]. The emission can then be collected by an infrared camera and the captured image reveals the solar cell's spatial defects and key electrical parameters [2]. Higher quality images provide more information which allows for more thorough image analyses [4]. However, these require expensive imaging systems with high quality cameras and optics.

Deep learning [5], also known as neural networks [6], is a type of machine learning algorithm that has seen incredible advancements over recent years [7]. This can be credited to improvements in technologies, such as the graphics processing unit, and a surge in open-source digital data [8, 9]. The large, complex neural network architecture enables the use of deep learning in computer vision, outperforming classical image processing algorithms such as bicubic interpolation filters used in image restoration [10]. Today, the use of deep learning includes medical classification [11], speech recognition [12], and many more [13, 14]. Deep learning has also been shown to be a powerful tool for denoising [13]. Specifically, as demonstrated by Lu et. al. [11], the deep learning architecture U-net [15] has outperformed other deep learning models in terms of being architecturally simple, yet effective, in denoising medical positron emission tomography (PET) images.

U-net models were first introduced by Ronneberger et al. [15]. They consist of a contracting path (encoder) and an expanding path (decoder). The encoder resembles a standard convolutional neural network (CNN) and the decoder mirrors the encoder. A key feature in this architecture is the skip connections between the same levels (the concatenations of the decoder with the corresponding layer from the encoder) – see Figure 1 [15].

In this study, we developed a U-net algorithm to significantly reduce the noise in EL images, enabling improvements in image quality without the need for expensive hardware or longer exposure times. This method presents a powerful approach to reducing the cost or to reducing measurement time (or a combination thereof) associated with EL imaging for solar cell and module inspection.

Methodology

For training the network, we used 7,680 EL images (520×520 pixels) of nine-busbar industrial state-of-the-art solar cells (~23% average efficiency). The trained network was then tested on 1,920 previously-unseen EL images of the same type of solar cells.

The dataset consisted of noisy images and their corresponding clean image for training and testing. Noisy images were created from the original ('clean') EL images by adding, to each of the images, both Poisson ('shot') noise of 10^6 photons, and Gaussian ('read') noise with a mean of 0 and a random variance between 0.0001 and 0.001 [16]. In EL systems, Poisson noise is produced due to the particle nature of photons that incident the camera while Gaussian noise is produced by conversion electronics in the sensor.

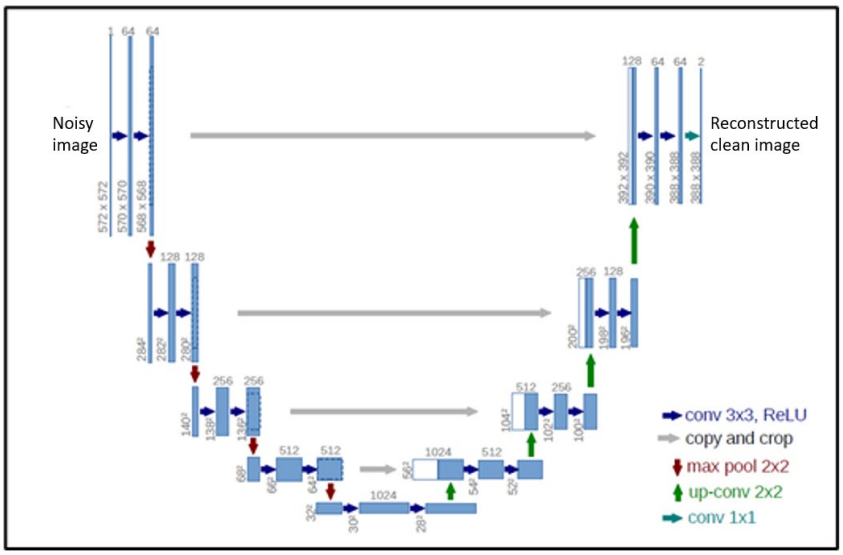

Figure 1. U-net architecture [13]

The U-net model used here was similar to Ronneberger et al. [13], however, the encoder was replaced with a pre-trained CNN "Resnet-34" [17] on 100,000 images across 200 classes. The library "fastai" was used to facilitate the creation, training, and testing of the models.

During training, the U-net model was trained in batches of four images at a time and the training images were cycled through 20 times (i.e., 20 epochs). The loss function used was the pixel-to-pixel mean squared error (MSE) as shown in Eq. (1).

$$\mathrm{MSE} = \frac{1}{N}\sum_{\mathrm{i}=1}^{N}(y_{\mathrm{i}} - \hat{y}_{\mathrm{i}})^2, \quad (1)$$

where N is the number of training examples, y_i is the original value, and $\hat{y}_i$ is the predicted value by the model.

To evaluate the performance of the developed model, the peak signal-to-noise ratio (PSNR) [18], structural similarity index metric (SSIM) [18, 19], and visual inspection were used to compare each reconstructed image to the corresponding original ('ground truth') image. PSNR measurements range from zero to infinity where a smaller value implies a lower image quality as there is a higher pixel difference between the two images. SSIM measures the similarity of visual features between the two images. The SSIM ranges from 0 to 1, where unity indicates that the two images are identical and zero indicates no structural similarity.

Results and Discussion

Figure 2(a) presents a representative clean EL image from the dataset while Figure 2(b) shows a noisy image created from the clean image. Figure 2(c) presents the U-net reconstructed clean image. These figures also feature a zoomed-in region for clarity in the visual inspection. It can be observed that the noisy image has a grainy appearance compared to the original clean image from the dataset. The PSNR of the noisy image was reduced to ~30.7 dB while its SSIM dropped to ~0.68. Examining the reconstructed image, it appears there is slightly less texture compared to the original. Furthermore, the reconstructed image clearly has little noise and includes all the key features of the original image, such as busbars, background luminescence, small defects, and measurement contacts. This is reflected in the significant improvements in the PSNR and SSIM of the noisy image, which increased by 30.3% and 39.6%, respectively.

As discussed, the developed U-net models were tested on 1,920 unseen EL solar cell images. Figure 3(a) and Figure 3(b) present the PSNR and SSIM distribution of the noisy and reconstructed images. The noisy images averaged a PSNR of 30.69 dB and an SSIM of 0.682. The reconstructed images averaged a PSNR of 40.01 dB and an SSIM of 0.950. Hence, the model improved the average PSNR of the noisy image by 30.4% and the average SSIM by 39.3%. The significant improvements in these noisy EL images demonstrate the viability of this deep learning approach. To further reinforce the effectiveness of this U-net model in denoising real-noisy images, its experimental validation will be presented at the conference.

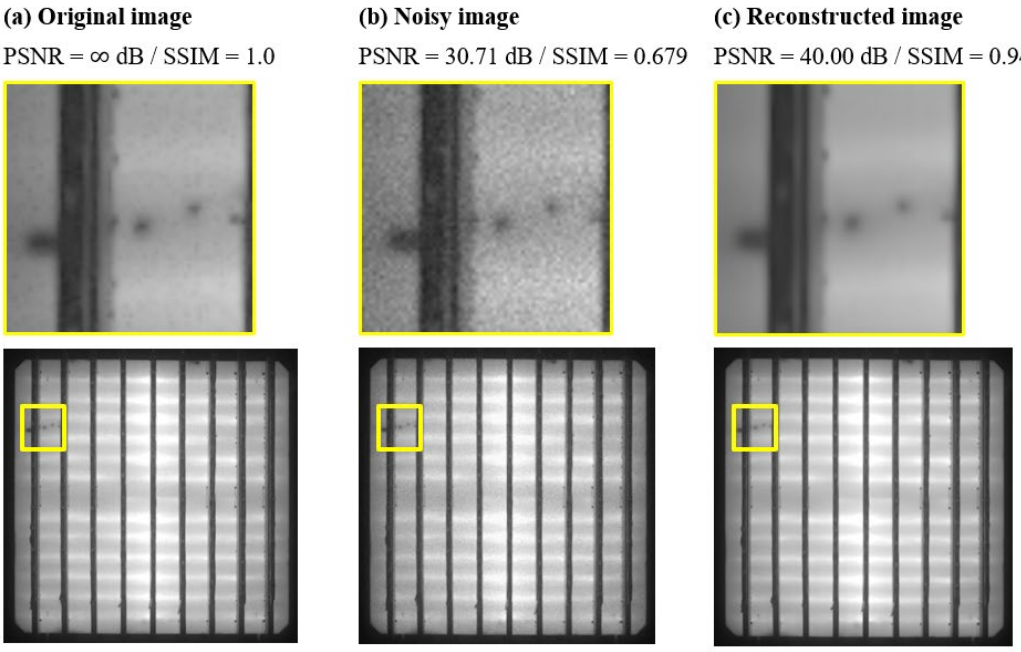

Figure 2. Denoising applied by the U-net approach: (a) a representative original image, (b) a noisy image, (c) and a reconstructed image. Their corresponding PSNR and SSIM are shown for quantitative comparison.

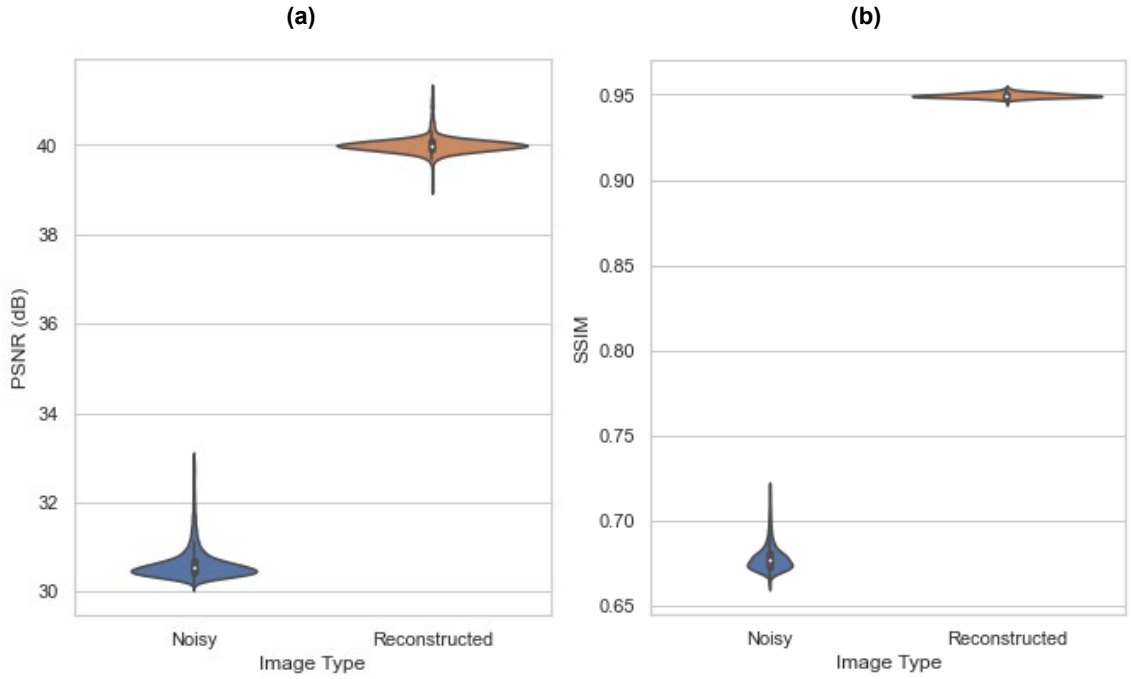

Figure 3. Violin graphs showing the distribution of (a) PSNR and (b) SSIM. The white diamond indicates the mean and the quartiles are shown by the vertical bar.

Conclusion

We present a novel deep learning U-net application that enables denoising and thereby significantly improves the quality of EL images. The developed U-net model successfully removed noise and improved the quality of the images with an increase of 30.4% in the PSNR metric and 39.3% in the SSIM. Its success is visually reflected in the reconstructed images, which have much better clarity than the noisy EL images and are near indistinguishable from the original EL images. These results highlight the significant potential of our approach in reducing the need for long exposure times (e.g., in outdoor photoluminescence imaging) or expensive EL imaging hardware to inspect PV devices, consequently, decreasing the overall cost of PV production.

References

[1] IRENA, 2019. 'Future of solar photovoltaic: Deployment, investment, technology, grid integration and socio-economic'.
[2] Fuyuki, T., Kondo, H., Yamazaki, T. & Takahashi, Y., 2005, 'Photographic surveying of minority carrier diffusion length in polycrystalline silicon solar cells by electroluminescence', *Appl. Phys. Lett.*, 86(26), p. 262108.
[3] Nair, G. B. & Dhoble, S. J., 2020, 'The fundamentals and applications of light-emitting diodes', *Series in Electronic and Optical Materials*, Woodhead Publishing.
[4] Bedrich, K. G., Bliss, M., Betts, T. R. & Gottschalg, R., 2015, 'Electroluminescence imaging of PV devices: determining the image quality', *42nd IEEE Photovoltaic Specialist Conference (PVSC),* pp. 1-5.
[5] LeCun, Y., Bengio, Y. & Hinton, G., 2015, 'Deep Learning', *Nature*, 521, pp. 436-444.
[6] Bingham, E., Kaski, S., Laaksonen, J. & Lampinen, J., 2015, 'Advances in Independent Component Analysis and Learning Machines', Academic Press.
[7] Saadat, M. & Shuaib, M., 2020, 'Advancements in deep learning theory and applications: perspective in 2020 and beyond', *Advances and Applications in Deep Learning*, Intechopen.
[8] Ng, A., 2017, 'Why is deep learning taking off?', Coursera.
[9] Sarker, I. H., 2021, 'Deep learning: a comprehensive overview on techniques, taxonomy, applications and research directions', *SN Computer Science*, 2, p. 420.
[10] Dwivedi, P., Chin, R. L., Trupke, T. & Hameiri, Z., 2022, 'A deep learning approach to increase luminescence image resolution of solar cells', *49th IEEE Photovoltaic Specialist Conference (PVSC).*
[11] Lu, W. et al., 2019. 'An investigation of quantitative accuracy for deep learning based', *Physics in Medicine and Biology*, 64(16), p. 165019.
[12] Zhang, Z. et al., 2018, 'Deep learning for environmentally robust speech recognition: an overview of recent developments', *ACM Transactions on Intelligent Systems and Technology*, 9(5), pp 1-28.
[13] Tian, C. et al., 2020, 'Deep learning on image denoising: An overview', *Neural Networks*, 131, pp. 251-275.
[14] Buratti, Y. et al., 2020, 'End-of-line binning of full and half-cut cells using deep learning on electroluminescence images', *47th IEEE Photovoltaic Specialists Conference (PVSC)*, pp. 133-138.
[15] Ronneberger, O., Fischer, P. & Brox, T., 2015, 'U-net: convolutional networks for biomedical image segmentation', *Medical Image Computing and Computer-Assisted Intervention (MICCAI)*, pp. 234-241.
[16] Zafirovska, I., 2019, 'Line scan photoluminescence and electroluminescence imaging of silicon solar cells and modules', PhD Thesis, the University of New South Wales.
[17] He, K., Zhang, X., Ren, S. & Sun, J., 2016, 'Deep residual learning for image recognition', *IEEE Conference on Computer Vision and Pattern Recognition (CVPR)*, pp. 770-778.
[18] Horé, A. & Ziou, D., 2010, 'Image quality metrics: PSNR vs. SSIM', 2010, *20th International Conference on Pattern Recognition*, pp. 2366-2369.
[19] Wang, Z., Bovik, A., Sheikh, H. R. & Simoncelli, E. P., 2004, 'Image quality assessment: from error visibility to structural similarity', *IEEE Transactions on Image Processing*, 13(4), pp. 600-612.